The role of high frequency modes in the plasma edge of W7-X

A. Krämer-Flecken[1], T. Andreeva[2], N. Chaudhary[2], A. Dinklage[2], G. Fuchert[2], J. Geiger[2], X. Han[3], M. Hirsch[2], G. Weir[2], T. Windisch[2], G. Wurden[4], H.M. Xiang[1,5] and the W7-X Team

[1]*Institut für Energie- und Klimaforschung, Forschungszentrum Jülich, Jülich, Germany*

[2]*Max Planck Institut für Plasmaphysik , Greifswald, Germany*

[3]*University of Wisconsin - Madison, Madison, WI 53706 USA*

[4]*Los Alamos National Laboratory, Los Alamos, NM, 87545, USA*

[5]*Institute of Plasma Physics, Chinese Academy of Sciences, Hefei, Anhui, PRC*

The superconducting stellarator W7-X is optimized with respect to minimize neoclassical transport. W7-X is equipped with an island divertor generating a $5/5$-island chain in the standard configuration ($\iota = 1$) at the plasma edge. Due to its flexibility in magnetic configurations the $5/5$-island chain can be produced in the scrape-off layer, but also in the plasma edge. The influence of an edge island chain on the confinement properties was already reported in W7-AS [1]. In the last two campaigns of W7-X several series of experiments have been performed [2] with the aim to investigate this influence on the confinement and to identify potential configurations for further scenario development towards a fusion reactor. For this purpose W7-X is equipped with high resolution turbulence diagnostics, amongst them a poloidal correlation reflectometry (PCR) yielding information on poloidal rotation and turbulence [3]. The PCR consists of a launching antenna (A) and 4 receiving antennae (B, C, D and E). It measures the fluctuations at a given cut-off layer by injecting microwaves within an appropriate frequency range.

Observations

In tab. 1 the normalized diamagnetic energy (W_{dia}) is shown as function of the magnetic configuration. Those configurations where the island chain is close to the last closed flux surface (LCFS), but still inside the plasma edge show an increased W_{dia}. The experiments suggest that the island position and its size/width are involved in the gain of W_{dia}. Furthermore, the increase of the confinement is accompanied by bursting instabilities [2] with sawtoothing behaviour showing an almost linear increase in W_{dia} with a sudden termination of the increase which is seen as spike in the plasma current signal (I_p) as shown in fig. 1.shown in fig 1. Here, the time trace of W_{dia} and the time derivative of I_p are shown. A threshold was set to identify the major spike in the I_p' signal and the dashed red lines show the coincidence of the crash in W_{dia} with the spike in I_p'. It is of interest to understand this process in more detail and look into the turbulence features during these events. The intermittent loss in W_{dia} is accompanied by a sudden drop of the electron temperature in the edge channels of the ECE-diagnostic [4].

Program	W_{dia} [kJ]	Config.	iota
221214.24	429	FLM000	1.057
221214.25	420	FMM003	1.057
221214.28	419	FMM002	1.057
221214.39	422	FMM001	1.064
221214.40	411	FMM000	1.070
221214.43	356	FNM001	1.070
221214.44	378	FOM004	1.100

Table 1: *Relevant programs and configuration from iota-Scan experiments*

In the cross spectral density spectra of the PCR a high frequency (HF) mode is detected as a shoulder at $f \approx -800\,\mathrm{kHz}$, shown in fig. 2. A clear variation in the power of the structure as well as in the frequency is observed. The mode is most prominent in the negative frequency branch as observed for the configuration FLM000, however, it is not the configuration where the maximum in W_{dia} is found. Also in the FLM000 case the center frequency of the mode is the smallest. More information on the mode is gained by calculating the coherence spectrum between two antennae, suppressing the uncorrelated background turbulence. The coherence spectrogram in fig. 3 is obtained for antennae D and E for the program 221214.25. The coherence is calculated for one scan of the PCR as indicated in the lower panel of the figure. A broad structure in the negative and positive frequency branch is observed. The mode structure is well separated from the low frequency turbulence, occupying a frequency range of $-300\,\mathrm{kHz}$ to $300\,\mathrm{kHz}$. Furthermore, the red solid line shows the temporal derivative of I_p. From fig. 3 several conclusion can be drawn: (i) the mode appears only in the narrow density window $2.3 \times 10^{19}\,\mathrm{m}^{-3}$ to $3.0 \times 10^{19}\,\mathrm{m}^{-3}$. And (ii) the mode activity is terminated by a spike in dI_p/dt, indicating a spike in W_{dia}. Due to missing of high temporal density profiles it is not clear whether the mode disappears or if the density profile undergoes a sudden change moving the density cut-off position into a region where no mode exists.

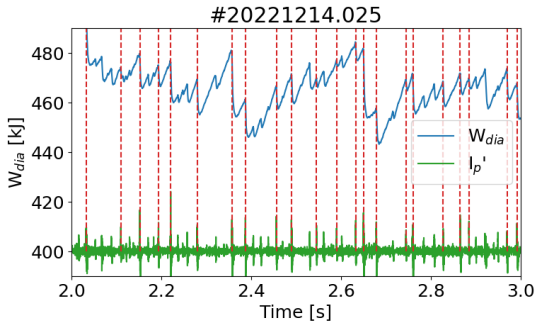

Figure 1: *W_{dia} and the derivative of I_p for a given time interval. Clearly seen is the correlation between the spikes on I_p and the crashes on W_{dia}*

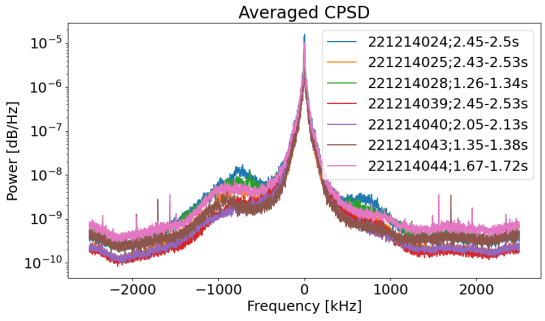

Figure 2: *PSD for experiment programs from table 1, showing the existence of high frequency modes at $f \approx 800\,\mathrm{kHz}$*

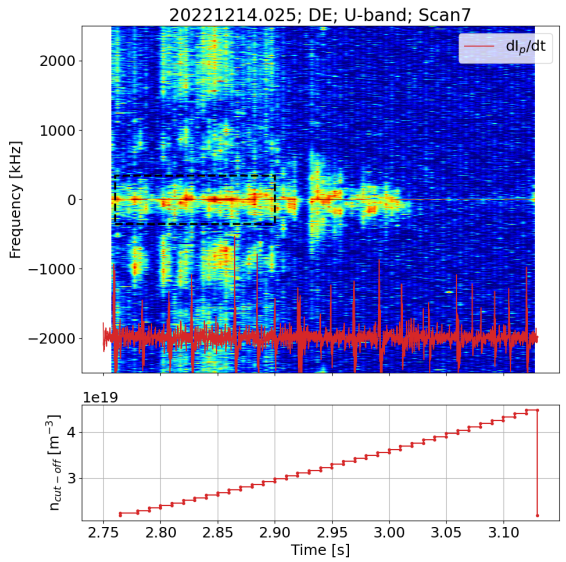

Figure 3: *Coherence spectrogram for antennae DE. The lower panel contains the cut-off density as function of time for one scan*

The general observations point into the direction that the improvement of the confinement is induced by the position of the 5/5-island chain. Therefore, the mode rotation with respect to the $E \times B$ rotation is analysed. From the evolution of the coherence in fig. 3 the $E \times B$-flow is limited to a frequency range of -350 kHz to 350 kHz, indicated by dashed box. The frequency range of the HF-mode is given by -1300 kHz to -400 kHz on the negative frequency branch. For both frequency intervals the cross correlation function (CCF) for the combination DE is calculated. According to the elliptical model [5] for the propagation of turbulence in general a measure for the delay time (Δt_c) is calculated as:

$$v_\perp \sim \frac{1}{\Delta t_c} = \frac{\Delta t}{(\Delta t^2 + \tau_0^2)} \tag{1}$$

Here, Δt denotes the time lag where the CCF has reached its maximum and τ_0 denotes the time lag, where the maximum of the CCF equals the auto correlation function. The calculation is performed for 1 ms time steps and averaged for time intervals with HF-mode activity.

In fig.4 the results for the programs 20221214.24 and .28 are presented, taking the poloidal distance of the antenna spots on the probed flux surface as constant. For both programs the $E \times B$-flow is much smaller than the value for the mode propagation which is interpreted that the mode propagation is in diamagnetic drift direction. This is a first evidence for a trapped electron mode (TEM).

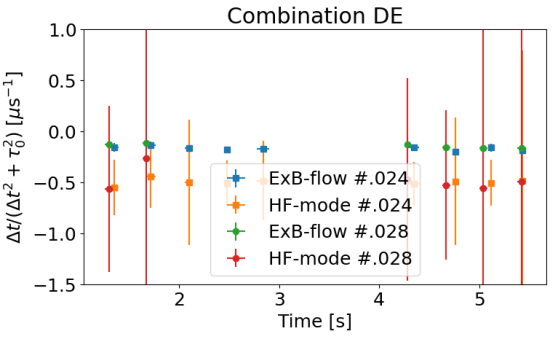

Figure 4: $1/\Delta t_c$ *for the time intervals with HF-modes for two programs.*

For the localization of the mode the program 20180927.22 from an iota-scan from a past campaign is analyzed. For mapping to R, profiles from Thomson Scattering (TS) are used, having in mind that TS measured across the X-point of the island in contrast to the PCR, measuring across the O-point. In Fig 5 the radial region, where HF-modes are observed, is marked as orange bar along the PCR line of sight (green line), together with the poloidal rotation profile shown as red squares. The Poincaré map in the background displays the position of one island

of the 5/5 island chain. The maximum of the mode activity is localized at the left end of the bar and indicates that the mode is located outside the island separatrix, taking into account that the radial uncertainty of the PCR is in the order of ± 5 mm. The distance of the island separatrix to the last closed flux surface (LCFS) is in all cases with mode activity ≤ 25 mm. Shifting the island further into the plasma, by increasing the edge iota extinguishes the HF-mode activity.

Discussion and Conclusions

As described above the HF-mode is related to the distance of the 5/5-island chain to the LCFS. It is assumed that with decreasing distance of the island separatrix to the LCFS the gradients in that region increase [4]. From a zeroth order approach the poloidal wave length of the HF-mode can be determined as s/m, where s is the poloidal circumference of a mean flux surface where the HF-mode is obtained and m is the mode number given as $m = s f_{HF}/v_{HF}$. From fig. 5 $v_\perp = -7.5\,\mathrm{km\,s^{-1}}$ is obtained for the $E \times B$-flow. From fig. 4, the ratio of HF-mode velocity to the $E \times B$-flow is ≈ 3. With these numbers the wave length amounts to $\approx$ 25 mm. Taking the averaged electron temperature $T_e = 280$ eV, $k_\perp \rho_* = 0.5$ is estimated. This value is in the range, usual covered by ITG- and TEM-modes, but, together with the higher velocity of the HF-mode it adds further evidence for a TEM nature of the HF-mode.

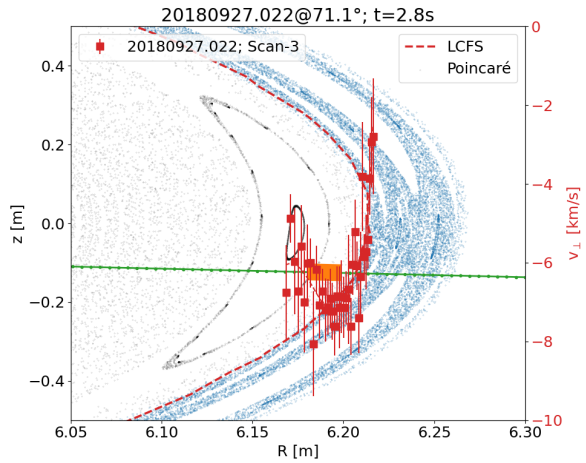

Figure 5: *$E \times B$-flow profile for FMM002. The dashed line marks the LCFS and the orange bar indicates the radial HF-mode range.*

Following the discussion J.Y. Kim [6] density gradient driven TEM modes (D-TEM) are most likely observed in tokamak plasmas. Moreover, this mode plays a dominant role in the L-H transition. In case D-TEM dominates in the plasma edge its growth rate will be reduced towards the SOL, where resistive ballooning modes (RBM) should dominate. Therefore the overall growth rate which is assumed to be proportional to the radial transport has a minimum which reduces the outward heat and particle transport. This mechanism may be responsible for the observed increase in W_{dia} in the iota scan experiments at W7-X.

References

[1] M. Hirsch, J. Baldzuhn, C. Beidler et al., Plasma Phys. and Control. Fusion **50** (2008) 053001, https://10.1088/0741-3335/50/5/053001
[2] T. Andreeva, J. Geiger, A. Dinklage et al., Nucl. Fusion **62** (2022) 026032, https://doi.org/10.1088/1741-4326/ac3f1b
[3] A. Krämer-Flecken, T. Windisch, W. Behr et al., Nucl. Fusion **57** (2017) 066023, https://doi.org/10.1088/1741-4326/aa66ae
[4] N. Chaudhary, M. Hirsch, T. Andreeva et al., The European Physical Journal Conferences 277 (2023) https://doi.org/10.1051/epjconf/202327703004
[5] G. He, G. Jin and Y. Yang, Annu. Rev. Fluid Mech. 2017. 49:51–70, https://doi.org/10.1146/annurev-fluid-010816-060309
[6] J.Y. Kim and H.S. Han, Phys. Plasmas **28**, 072509 (2021), https://doi.org/10.101063/5.0053455